

## Langevin equations and computed correlation functions for a rotating and translating asymmetric top

M. W. Evans

*Department of Physics, University College of Swansea, Singleton Park, Swansea SA2 8PP, Glamorgan, United Kingdom*

G. J. Evans

*Department of Chemistry, The University College of Wales, Aberystwyth SY23 1NE, Dyfed, United Kingdom*

(Received 2 July 1985; revised manuscript received 11 February 1986)

The three-dimensional diffusion in condensed material of a rotating and translating asymmetric-top molecule is considered with use of three frames of reference: the laboratory frame  $(x, y, z)$ , a rotating frame  $(1, 2, 3)'$ , and a moving frame  $(1, 2, 3)$ . The frame  $(1, 2, 3)'$  has the same origin as  $(x, y, z)$ , but rotates with an angular velocity  $\omega$ , the molecular angular velocity. The frame  $(1, 2, 3)$  is defined by the principal molecular moments of inertia, and its origin is therefore the molecular center of mass. The molecular angular velocity  $\omega$  is the same in all three frames. By writing a pair of simultaneous single-molecule Langevin equations, a rotational equation in  $(1, 2, 3)$  and a translational equation in frame  $(1, 2, 3)'$ , a natural description of the molecular diffusion is obtained without the need of friction cross terms. This description introduces into the analysis the center-of-mass position vector  $\mathbf{r}$ , and the forces obtained by transforming Newton's equation into a noninertial frame, i.e., by the frame transformation  $(x, y, z) \rightarrow (1, 2, 3)'$  or vice versa. These are the Coriolis force  $2m\omega \times \mathbf{v}$ , the centripetal force  $m\omega \times (\omega \times \mathbf{r})$ , and the force  $m\dot{\omega} \times \mathbf{r}$ . The analysis also implies the consideration of the velocity  $\omega \times \mathbf{r}$ . Here  $\mathbf{v}$  is the molecular center-of-mass linear velocity,  $\omega$  the angular velocity, and  $\mathbf{r}$  the position vector of the center of mass. It is shown by computer simulation that autocorrelation and cross-correlation functions of these terms can exist *both* in frame  $(x, y, z)$  and in frame  $(1, 2, 3)$ , the moving frame. Examples are provided in the liquid state for the achiral asymmetric top dichloromethane and for the enantiomers and racemic mixture of bromochlorofluoromethane at two state points. The symmetry properties of some of the new cross-correlation functions are tabulated. Finally, experimental methods are suggested for observing cross-correlation functions such as these and for testing experimentally the detailed numerical paradigm provided by these computer simulations. Examples of one method are given with reference to the far-infrared power absorption of the tris(acetylacetonate) complexes of cobalt and chromium in the powdered crystalline state.

### INTRODUCTION

The computer simulation<sup>1</sup> of molecular dynamics in the condensed states of matter now allows the investigation of many details that are obscured in the conventional theory of molecular diffusion.<sup>2</sup> At a fundamental level, it is necessary to take into account the fact that, in general, diffusing molecules (neglecting vibration) both rotate *and* translate. The historical approach has relied on the "factorization" of the molecular dynamics into "purely" rotational and "purely" translational components. This achieves a considerable mathematical simplification but, as we point out in this paper, loses most of the available statistical information. For example, the standard translational or rotational Langevin equations<sup>2</sup> cannot be used to establish the nature of the statistical correlation *between* rotation and translation on the basic, single-molecule, level. This has opened a big gap between hydrodynamics and molecular dynamics which continues to exist to this day. It is necessary to use computer simulation to begin to fill this gap because of the increasingly important role<sup>3</sup> played by Langevin dynamics in the theory of flocculation, sedimentation of lyotropic liquid crystals,<sup>4</sup> and colloid dynamics. It is essential to clarify matters at

a one-molecule level before developing techniques to deal with two-, three-, and  $N$ -molecule rotational-translational Langevin dynamics.

It is not obvious to us that the Langevin equation for one-molecule "rotation-translation" has been written down as clearly as possible. Several papers on the subject are available in the literature, all of which attain a high level of mathematical complexity but which contain flaws because the phenomenology [i.e., the (then) unavoidable guess work] has not stood up to the test of time. An example is the first substantial paper on this subtle and difficult subject: that of Condiff and Dahler.<sup>5</sup> They seem to have written a pair of interlinked Langevin equations to which give, in the laboratory frame, the result

$$\langle \mathbf{v}(t)\omega^T(0) \rangle \neq 0, \quad t > 0. \quad (1)$$

Equation (1) is now known to contradict the Berne-Pecora theorem<sup>6</sup>

$$\langle \mathbf{v}(t)\omega^T(0) \rangle = 0, \quad \text{for all } t. \quad (2)$$

Here  $\mathbf{v}$  is the molecular center-of-mass linear velocity, and  $\omega$  is the angular velocity of the *same* molecule. Equation (2) follows because the sign of  $\mathbf{v}$  is reversed by parity

reversal, whereas that of  $\omega$  remains the same.

The most complete theory seems to be that of Steiger and Fox,<sup>7</sup> whose results have recently been generalized to include the memory-function hierarchy by Grigolini and co-workers.<sup>8</sup> Steiger and Fox suggest that there may be some mathematical inconsistencies in the earlier papers by Evans<sup>9</sup> and by Hwang and Freed,<sup>10</sup> and write down formal equations of great complexity both for single-molecule and  $N$ -molecule dynamics.

However, except in one very special case, they do not seem to have attempted a solution of these  $N$ -particle equations, either with computer simulation or with analytical techniques.

A recent review article by Dickinson<sup>3</sup> has emphasized the importance of Langevin dynamics in several fields of physics and chemical physics, but it seems that the nature of the cross-correlation functions between rotational and translational modes of motion has not come to light from analytical considerations of the simplest type of Langevin equation—that for one Brownian particle.

In this paper this equation is written in Sec. I for an asymmetric top rotating and translating in three dimensions. It is necessary to write this equation in rotating frames of reference,<sup>11,12</sup> and this introduces terms which are shown by computer simulation to lead to new ways of measuring the correlation between molecular rotation and translation, and to new autocorrelation functions in rotating and laboratory frames of reference which do not appear in the "decoupled" Langevin equations describing rotation and translation separately.<sup>2</sup>

In Sec. II these new cross-correlation functions are illustrated by computer simulation with reference to 108  $\text{CH}_2\text{Cl}_2$  molecules at 296 K in the liquid state at equilibrium and in the presence of a strong,  $z$  axis, external, electric field. Such a field is known to break the parity-reversal rule<sup>6,13</sup> which leads to Eq. (2) and in this way introduces new cross correlations<sup>14</sup> in the laboratory and rotating frames of reference. Results from computer simulation are also provided for enantiomers and racemic mixture of the chiral bromochlorofluoromethanes.

In Sec. III, finally, we suggest experimental methods, based on spectra for chiral liquids and solids and on electric-field-induced birefringence, to detect these new cross correlations in the laboratory frame of reference.

### I. CROSS-CORRELATION FUNCTIONS BETWEEN ROTATIONAL AND TRANSLATIONAL MODES OF MOTION

The Langevin equation for the decoupled rotational diffusion of an asymmetric top in three dimensions is well known<sup>2</sup> to be (in component form)

$$\begin{aligned} I_1 \dot{\omega}_1 - (I_2 - I_3) \omega_2 \omega_3 + I_1 \beta_1 \omega_1 &= I_1 \dot{W}_1, \\ I_2 \dot{\omega}_2 - (I_3 - I_1) \omega_3 \omega_1 + I_2 \beta_2 \omega_2 &= I_2 \dot{W}_2, \\ I_3 \dot{\omega}_3 - (I_1 - I_2) \omega_1 \omega_2 + I_3 \beta_3 \omega_3 &= I_3 \dot{W}_3, \end{aligned} \quad (3)$$

where  $I_1$ ,  $I_2$ , and  $I_3$  are the three principal moments of inertia,  $\omega_1$ ,  $\omega_2$ , and  $\omega_3$  are components of the molecular angular velocity in the moving frame of reference (1,2,3)

defined by the axes of the three principal moments of inertia and whose origin is at the molecular center of mass. The three friction coefficients  $\beta_1$ ,  $\beta_2$ , and  $\beta_3$  are properties of the molecule, defined by the molecular symmetry alone, and are scalars, invariant—to frame transformation. They are assumed to be diagonal in the same frame as  $I_1$ ,  $I_2$ , and  $I_3$  in the standard theory of rotational diffusion.<sup>2</sup> The Wiener processes  $\dot{W}_1$ ,  $\dot{W}_2$ , and  $\dot{W}_3$  are defined as being, in frame (1,2,3), statistically independent, so that for  $I_1 = I_2 = I_3$  (the spherical top), the three equations reduce to one:

$$\dot{\omega} + \beta \omega = \dot{W}. \quad (4)$$

If the center of mass of the molecule is moving in the laboratory frame there is an additional degree of "diffusional freedom" and Eqs. (3) must be supplemented to take account of this fact. This is our point of departure from the conventional theory of molecular diffusion because we write the supplementary translational Langevin equation as

$$\dot{\mathbf{v}} + 2\boldsymbol{\omega} \times \mathbf{v} + \dot{\boldsymbol{\omega}} \times \mathbf{r} + \boldsymbol{\omega} \times (\boldsymbol{\omega} \times \mathbf{r}) + \beta_v (\mathbf{v} + \boldsymbol{\omega} \times \mathbf{r}) = \dot{\mathbf{W}}_{vm}. \quad (5)$$

Equation (5) is written in a rotating frame of reference whose origin is coincident with that of frame  $(x,y,z)$ . We denote this frame of reference by  $(1,2,3)'$ . It is generated from the standard laboratory frame translational Langevin equation by<sup>15</sup>

$$[\dot{\mathbf{v}}]_{(x,y,z)} = [\dot{\mathbf{v}} + 2\boldsymbol{\omega} \times \mathbf{v} + \dot{\boldsymbol{\omega}} \times \mathbf{r} + \boldsymbol{\omega} \times (\boldsymbol{\omega} \times \mathbf{r})]_{(1,2,3)'}, \quad (6)$$

$$[\mathbf{v}]_{(x,y,z)} = [\mathbf{v} + \boldsymbol{\omega} \times \mathbf{r}]_{(1,2,3)'}, \quad (7)$$

$$[\dot{\mathbf{r}}]_{(1,2,3)'} = [\mathbf{v}]_{(1,2,3)'}$$

In these equations

$$[\boldsymbol{\omega}]_{(x,y,z)} = [\boldsymbol{\omega}]_{(1,2,3)'} \quad (8)$$

is the molecular angular velocity, which is the same in all three frames because  $\boldsymbol{\omega}$  is also the angular velocity of frames (1,2,3) or (1,2,3)' with respect to frame  $(x,y,z)$ . This quantity appears in both the translational equation (5), and the rotational equations (3). Therefore the complete description of the rotational and translational molecular diffusion in terms of one-particle Langevin dynamics involves solving these equations *simultaneously*.

This is a formidable analytical problem,<sup>2</sup> but considerable progress can be made with the aid of conventional computer simulation,<sup>1</sup> the subject of this paper.

The first step in this direction involves the recognition of the existence in the frames (1,2,3) and  $(x,y,z)$  of numerous auto and cross-correlation functions suggested by the terms in Eqs. (6) and (7). In this respect these equations suggest the existence of time autocorrelation functions (ACF's) between the Coriolis acceleration  $[2\boldsymbol{\omega} \times \mathbf{v}]_{(1,2,3)}$  the "nonuniform" acceleration  $[\dot{\boldsymbol{\omega}} \times \mathbf{r}]_{(1,2,3)}$  and the centripetal acceleration  $[\boldsymbol{\omega} \times (\boldsymbol{\omega} \times \mathbf{r})]_{(1,2,3)}$  together with the ACF of the velocity  $[\boldsymbol{\omega} \times \mathbf{r}]_{(1,2,3)}$ .

The existence of all these autocorrelation functions is confirmed in this paper using the technique of conventional and field-on<sup>16</sup> computer simulation for the asym-

metric tops dichloromethane and bromochlorofluoromethane in the liquid state. As far as we know there is no simple analytical method available for their analysis, and the only way to progress in this area is to solve equations such as (3) and (5) on a computer.

Another important point is that *these correlation functions also exist in the laboratory frame of reference*  $(x,y,z)$ . This becomes clear because the frame transformations [Eqs. (6) and (7)] are *reversible*:

$$[\dot{\mathbf{v}}]_{(1,2,3)'} = [\dot{\mathbf{v}} + 2\boldsymbol{\omega} \times \mathbf{v} + \dot{\boldsymbol{\omega}} \times \mathbf{r} + \boldsymbol{\omega} \times (\boldsymbol{\omega} \times \mathbf{r})]_{(x,y,z)}, \quad (9)$$

$$[\mathbf{v}]_{(1,2,3)'} = [\mathbf{v} + \boldsymbol{\omega} \times \mathbf{r}]_{(x,y,z)}; \quad (10)$$

using the results

$$\langle \mathbf{v}(t) \cdot \mathbf{v}(0) \rangle_{(1,2,3)'} \neq 0, \quad (11)$$

$$\langle \dot{\mathbf{v}}(t) \cdot \mathbf{v}(0) \rangle_{(1,2,3)'} \neq 0,$$

it follows that numerous laboratory-frame autocorrelation and cross-correlation functions must exist on the basis of the elementary frame transformations (9) and (10). These have not been explored before, and it is not clear to the present authors whether the available literature indicates their existence or not.

We introduce the use of *two* rotating frames,  $(1,2,3)$  and  $(1,2,3)'$ , in order to try to clarify a difficult dynamical problem. In this context we note that the frames  $(1,2,3)$  and  $(1,2,3)'$  do not rotate with respect to each other. An observer rotating with the frame  $(1,2,3)'$  would see *only the translational motion* of the center of mass of each molecule, with the rotational motion "filtered out." In the frame  $(1,2,3)'$  the Langevin equation describing this filtered out or "residual" translational motion is Eq. (5). The  $\boldsymbol{\omega}$  term in this equation appears because the frame  $(1,2,3)'$  is rotating with respect to an observer in the laboratory frame  $(x,y,z)$  at an angular velocity  $\boldsymbol{\omega}$ . This is also the angular velocity of the frame  $(1,2,3)$  with respect to  $(x,y,z)$ , i.e., the molecular angular velocity itself. The following is therefore true:

$$[\boldsymbol{\omega}]_{(1,2,3)} = [\boldsymbol{\omega}]_{(1,2,3)'} = [\boldsymbol{\omega}]_{(x,y,z)},$$

i.e.,  $\boldsymbol{\omega}$  is the same in all three frames.

The presence of  $\boldsymbol{\omega}$  in a *translational* equation [Eq. (5)] is explained naturally by the fact that the molecules are also rotating;  $\boldsymbol{\omega}$  is therefore governed simultaneously by *two* equations [Eqs. (3) and Eq. (5)]: The diffusing molecule is rotating in frame  $(x,y,z)$ , and its center of mass is also translating in frame  $(x,y,z)$ . However, in frame  $(1,2,3)$ , which has its origin at the molecular center of mass, the translational motion cannot be discerned, and in consequence there is *no direct* translational term in Eq. (3). Therefore, *quid erat demonstrandum*, the molecular diffusion is described *completely*, in the context of the simplest type of Langevin equation, by the simultaneous use of Eq. (3) in frame  $(1,2,3)$  and Eq. (5) in frame  $(1,2,3)'$ . There is, apparently, *no need* for the friction cross terms that have appeared in almost all the papers on this subject known to us.<sup>17</sup> Therefore the simultaneous use of Eqs. (3) and (5) both clarifies and simplifies the general problem of the diffusing asymmetric top.

It is relatively straightforward to build up the auto-

correlation and cross-correlation functions suggested by the structure of these equations by standard running-time averaging<sup>1,2</sup> on data from computer simulation.

#### A. Digital computer simulations of cross-correlation functions

The first liquid-state cross-correlation function between linear center of mass velocity  $\mathbf{v}$  and angular velocity  $\boldsymbol{\omega}$  was detected by Ryckaert, Bellemans, and Ciccotti<sup>11</sup> in 1981. In order to detect this they had to use the moving frame of reference  $(1,2,3)$ , because the simple cross-correlation function used in their work, i.e.,

$$\langle \mathbf{v}(t) \boldsymbol{\omega}^T(0) \rangle$$

vanishes for all  $t$  in frame  $(x,y,z)$ . Therefore, although it may be obvious that the molecules in a liquid must have their rotational and translational motion correlated statistically, it is not at all obvious how. Furthermore, only a few off-diagonal elements of the matrix  $\langle \mathbf{v}(t) \boldsymbol{\omega}^T(0) \rangle_{(1,2,3)}$ , discovered by Ryckaert *et al.*, exist. In the case of the molecule  $\text{CH}_2\text{Cl}_2$ , for example, only two exist. Therefore it is necessary to be careful what frame one works in to see anything at all, and it is significant in this context that analytical theory prior to 1981 *was not able* to predict the results obtained by Ryckaert *et al.* using molecular-dynamics computer simulation.<sup>18</sup> Therefore, to obtain even the most basic theoretical knowledge of this type of cross correlation in liquids, the choice of frame is critically important. Autocorrelations, such as those of  $2\mathbf{v} \times \boldsymbol{\omega}$ ,  $\boldsymbol{\omega} \times \mathbf{r}$ , and  $\boldsymbol{\omega} \times (\boldsymbol{\omega} \times \mathbf{r})$ , exist, however, in both frames, as reported elsewhere<sup>19</sup> and in this case the frame transformation provides a little less insight. Autocorrelation functions *always* exist in all three frames,  $(1,2,3)$ ,  $(x,y,z)$ , and  $(1,2,3)'$ .

The existence of cross correlations in the moving frame is basically the reason why the translational Langevin equation, well known in the laboratory frame, has to be put in the unwieldy and highly nonlinear form of Eq. (5), and solved simultaneously with Eq. (3). If this is not done, there can be no analytical explanation of the large bulk<sup>20</sup> of results on cross correlations already available from computer simulation in terms of Langevin dynamics.

In addition to this, further insights have become available recently about what can be learned *experimentally* about the role of cross correlations in condensed matter.

Perhaps the most important of these is that cross-correlation functions must be used<sup>12</sup> to explain why a spectral band shape of an enantiomer (a left- or right-handed molecule) is different from that of a racemic mixture. This very well known<sup>21</sup> experimental observation has no natural explanation in terms of Langevin dynamics—an oversight which was corrected only by the discovery, by computer simulation in 1983, that two elements of the *moving* frame matrix  $\langle \mathbf{v}(t) \boldsymbol{\omega}^T(0) \rangle$  *mirror each other in time dependence* for a left- and right-handed molecule, and disappear for all  $t$  in the 50/50 (racemic) mixture.<sup>12</sup> If we had restricted ourselves to an analysis in the laboratory frame  $(x,y,z)$  we would not have been able to offer *any* explanation for this experimental observation.

because in frame  $(x,y,z)$  the simple matrix  $\langle v(t)\omega^T(0) \rangle$  vanishes for all  $t$  for the right-hand molecule, the left-hand molecule, and the mixture. The exclusive use of the laboratory frame in this case therefore leads us nowhere. This is consistent with the well-known observation that the physical properties of a right-hand and left-hand molecule in the frame  $(x,y,z)$  are always identical. In the moving frame (1,2,3), this is no longer true.

Secondly, it has been discovered, again by computer simulation,<sup>22,23</sup> that an external electric field promotes the existence of two off-diagonal elements of  $\langle v(t)\omega^T(0) \rangle$  directly in frame  $(x,y,z)$ . For a  $z$ -axis field these are  $(x,y)$  and  $(y,x)$ . Again, there was no indication of this from the analytical theory prior to its discovery, numerically, in 1985. This is another clear indication, therefore, of the need for a new approach to the Langevin equations themselves. The experimental importance of this electric field effect is that it allows, in principle, the isolation of cross correlations from autocorrelation functions using techniques such as electric-field-induced birefringence.

So far, we have restricted the discussion to only one type of cross-correlation function  $\langle v(t)\omega^T(0) \rangle$ . The structure of Eqs. (3) and (5) suggests, however, the existence of several more. Without actually solving these equations, the technique of computer simulation is used in this paper to establish the existence or otherwise of these cross-correlation functions in frames (1,2,3) and  $(x,y,z)$  and in the presence and absence of the electric field  $E$ . It is shown in this paper that cross correlation is a highly selective phenomenon, only a very few out of the types allowed by the terms in Eqs. (3) and (5) exist. Each and every one of these types could be extracted by the combined use of spectroscopy, electric fields, chiral materials, and computer simulation. Typically, spectral data from various sources would be matched as closely and as self-consistently as possible using computer simulation, in the presence and absence of the electric field, and the trajectories thus defined used to construct the cross-correlation functions.

Without wishing to become too speculative, the rapidly developing technique of analogue circuit simulation<sup>24-26</sup> could be used to solve Eqs. (3) and (5) directly, and the cross-correlation functions from the analogue and digital simulations compared directly. After this, direct comparison between analytical theory and experimental data would be made.

The various autocorrelation and cross-correlation functions computed in this paper are all constructed from the terms appearing in Eqs. (3) and (5), and are as follows.

(1) The autocorrelation functions of  $2v \times \omega$ ,  $\dot{\omega} \times r$ , and  $\omega \times (\omega \times r)$ .

(2) Cross-correlation functions, namely,

$$\begin{aligned} \text{(i)} & \frac{\langle 2v(t) \times \omega(t) \cdot \dot{\omega}(0) \times r(0) \rangle}{2 \langle \omega^2(0) \rangle^{1/2} \langle v^2(0) \rangle^{1/2} \langle \dot{\omega}^2(0) \rangle^{1/2} \langle r^2(0) \rangle^{1/2}}, \\ \text{(ii)} & \frac{\langle 2v(t) \times \omega(t) \cdot \omega(0) \times [\omega(0) \times r(0)] \rangle}{2 \langle \omega^2(0) \rangle^{1/2} \langle v^2(0) \rangle^{1/2} \langle \omega^2(0) \rangle \langle r^2(0) \rangle^{1/2}}, \\ \text{(iii)} & \frac{\langle 2\omega(t) \times v(t) \cdot v(0) \rangle}{2 \langle \omega^2(0) \rangle^{1/2} \langle v^2(0) \rangle}, \end{aligned}$$

$$\begin{aligned} \text{(iv)} & \frac{\langle 2v(t) \times \omega(t) \cdot \omega(0) \times r(0) \rangle}{2 \langle \omega^2(0) \rangle \langle v^2(0) \rangle^{1/2} \langle r^2(0) \rangle^{1/2}}, \\ \text{(v)} & \frac{\langle r(t) \times \dot{\omega}(t) \cdot \omega(0) \times [\omega(0) \times r(0)] \rangle}{\langle \dot{\omega}^2(0) \rangle^{1/2} \langle \omega^2(0) \rangle \langle r^2(0) \rangle}, \\ \text{(vi)} & \frac{\langle \dot{\omega}(t) \times r(t) \cdot v(0) \rangle}{\langle \dot{\omega}^2(0) \rangle^{1/2} \langle r^2(0) \rangle^{1/2} \langle v^2(0) \rangle^{1/2}}, \\ \text{(vii)} & \frac{\langle r(t) \times \dot{\omega}(t) \cdot \omega(0) \times r(0) \rangle}{\langle \dot{\omega}^2(0) \rangle^{1/2} \langle r^2(0) \rangle \langle \omega^2(0) \rangle^{1/2}}, \\ \text{(viii)} & \frac{\langle \omega(t) \times [\omega(t) \times r(t)] \cdot v(0) \rangle}{\langle \omega^2(0) \rangle \langle r^2(0) \rangle^{1/2} \langle v^2(0) \rangle^{1/2}}, \\ \text{(ix)} & \frac{\langle \omega(t) \times [\omega(t) \times r(t)] \cdot r(0) \times \omega(0) \rangle}{\langle \omega^2(0) \rangle^{1/2} \langle \omega^2(0) \rangle \langle r^2(0) \rangle}, \\ \text{(x)} & \frac{\langle v(t) \cdot \omega(0) \times r(0) \rangle}{\langle v^2(0) \rangle^{1/2} \langle \omega^2(0) \rangle^{1/2} \langle r^2(0) \rangle^{1/2}}. \end{aligned}$$

A full theory of the diffusing asymmetric top must therefore produce self-consistently all these correlation functions in any frame of reference.

Experimental confirmation of the existence of cross-correlation functions such as  $\langle v(t)\omega^T(0) \rangle$  has recently been shown<sup>12</sup> to be possible by comparing spectra of individual enantiomers (optically active liquids) with that of their equimolar (racemic) mixture. The matrix  $\langle v(t)\omega^T(0) \rangle$  exists for  $0 < t < \infty$  in the frame (1,2,3). It has been demonstrated by computer simulation<sup>16,18</sup> that two well-defined off-diagonal elements switch sign in one enantiomer (e.g., the  $R$  enantiomer) compared with the other. These cross-correlation functions are therefore "mirror-image" functions of time. They disappear for all  $t$ , however, in the equimolar solution (racemic mixture). In terms of molecular dynamics, therefore, there is a difference in the statistical behavior of two enantiomers in frame (1,2,3), a difference which shows up in the symmetry of the matrix  $\langle v(t)\omega^T(0) \rangle_{(1,2,3)}$  and similar tensor cross-correlation functions.

In terms of molecular dynamics, this is the only possible reason why unpolarized spectra such as conventional far infrared power absorption can be, and are, different in an enantiomer and a racemic mixture, but are always identical in the two enantiomers.

The Fourier transform of the frequency-dependent far infrared power absorption is always a time-correlation function,<sup>2</sup> and this difference can always be traced, with the aid of computer simulation, to the cross-correlation functions such as  $\langle v(t)\omega^T(0) \rangle$  that are, in molecular dynamical terms, responsible for the difference. This theorem is perfectly general, and is applicable to condensed chiral matter—liquids, liquid crystals,<sup>4</sup> molecular crystals, chiral polymers, amorphous chiral solids, and so on. In this paper it is demonstrated experimentally with reference to the  $\Delta$  and  $\Lambda$  enantiomers of the tri(acetyl acetate) complexes of cobalt and chromium and their respective racemic mixtures in the solid state. The far-infrared power-absorption spectrum of the  $\Delta$  and  $\Lambda$  enantiomers are identical within the experimental uncertainty, but that of the racemic mixture is distinctly and obviously different. The spectra are reported for powdered crystal-

line samples in Sec. III.

We also demonstrate the theorem computationally in Sec. II with reference to several new autocorrelation and cross-correlation functions of the enantiomers and racemic mixture of bromochlorofluoromethane.<sup>27</sup> For example, the autocorrelation functions of the Coriolis and centripetal accelerations are different in frame  $(x,y,z)$  for enantiomer and mixture. Particularly subtle insights<sup>12</sup> are given by using the moving frame (1,2,3) for both autocorrelation and cross-correlation functions. Comparisons with functions of this kind are made for the enantiomers and the racemic mixture. These comparisons show clearly that as soon as we start to consider rotation superimposed on translation, *a great amount of new information becomes available*. This can be established with the aid of computer simulation, but it also becomes clear that the well-known differences in the infrared spectra and general physical properties of enantiomers and their racemic mixture can, and must, be traced to *cross-correlation functions of time*. There is no way of explaining the fundamental dynamical properties of condensed chiral matter without this realization. This is also true for any spectroscopic techniques capable<sup>2,8,18</sup> of providing information on the molecular dynamics of chiral materials.

## II. COMPUTER SIMULATION METHODS

### A. Liquid dichloromethane

The ensemble considered in the computer simulation<sup>16</sup> consisted of 108  $\text{CH}_2\text{Cl}_2$  molecules modeled with a  $3 \times 3$  site-site potential made up of Lennard-Jones and partial-charge terms as follows:

$$\frac{\epsilon(\text{CH}_2\text{-CH}_2)}{k} = 70.5 \text{ K}, \quad \sigma(\text{CH}_2\text{-CH}_2) = 3.96 \text{ \AA},$$

$$q_{\text{CH}_2} = 0.302 |e|, \quad \frac{\epsilon(\text{Cl-Cl})}{k} = 173.5 \text{ K},$$

$$\sigma(\text{Cl-Cl}) = 3.35 \text{ \AA}, \quad q_{\text{Cl}} = -0.151 |e|.$$

The  $\text{CH}_2$  group is therefore represented very simply as a unit of mass 14, with two Cl atoms of mass 35.5 each. The molar volume used was  $8.0 \times 10^{-5} \text{ m}^3$  at 296 K.

In order to build up the correlation functions 2700 time steps were used, each of  $5.0 \times 10^{-15} \text{ s}$ . One segment for the correlation-function computation therefore consisted of 900 records, each separated by three time steps.

Each correlation function was computed both in the molecular moment of inertia frame<sup>11,16</sup> (1,2,3) and the laboratory frame  $(x,y,z)$ , using a running-time average<sup>1,2</sup> over data stored on disk or magnetic tape on Control Data

Corporation CDC-7600 and Cyber-205 computers.

The simulations were repeated with an intense electric field of force in the  $z$  axis of the laboratory frame, using the recently developed technique of field-on computer simulation, as described elsewhere.<sup>16</sup> After applying the field, heating effects, if any, introduced by the presence of a constant external electric field of force are dissipated using the standard methods of molecular-dynamics simulation.<sup>1,16</sup> The standard temperature rescaling routine was utilized with the temperature allowed to fluctuate by 25 K either side of the mean input temperature of 296 K. Therefore after equilibrium has been reached in the field-on case there are no extraneous heating effects, other than those normally encountered in the standard simulation method. The only effect of the electric field is to increase the potential energy, i.e., to make it less negative.<sup>22</sup> The kinetic energy remains the same in the field-off and field-on cases because the sample is thermostated by the temperature-rescaling routine.

The effect of an external electric field of this kind is to break the symmetry of the Hamiltonian to parity reversal. This invalidates the Berne-Pecora theorem<sup>6</sup> [Eq. (2)] and means, in effect, that time correlation functions may exist<sup>22</sup> in frames  $(x,y,z)$  or (1,2,3) in the presence of an electric field that would vanish otherwise. This is crucial in devising an actual experimental method to probe the nature of specific cross-correlation functions between rotation and translation, as shown later in this paper. In the following section the correlation functions described above are illustrated in the field-off case, and at field-on equilibrium in the presence of an electric field<sup>22</sup> strong enough nearly to saturate the Langevin function. A field of this strength helps to define the extra effects more clearly and to cut down the "statistical noise" defined as the difference between consecutive segments in computed correlation functions.

### B. The enantiomers and racemic mixture of liquid bromochlorofluoromethane

It has been shown recently<sup>12</sup> that the comparison of spectra from enantiomers and their racemic mixture provides information on the matrix correlation  $\langle \mathbf{v}(t) \omega^T(0) \rangle_m$  in the moving frame of reference, because two elements out of nine in matrices of this type are mirror images for the  $R$  and  $S$  enantiomers and disappear in the mixture.<sup>18</sup> For the purposes of investigating the new correlation functions derived in this paper the  $R$  and  $S$  enantiomers and racemic mixture of bromochlorofluoromethane<sup>27</sup> were simulated with a  $5 \times 5$  site-site potential consisting of atom-atom terms and point charges as follows:

$$\epsilon(\text{C-C})/k = 35.8 \text{ K}, \quad \sigma(\text{C-C}) = 3.4 \text{ \AA}, \quad q_{\text{C}} = 0.335 |e|,$$

$$\epsilon(\text{H-H})/k = 10.0 \text{ K}, \quad \sigma(\text{H-H}) = 2.8 \text{ \AA}, \quad q_{\text{H}} = 0.225 |e|,$$

$$\epsilon(\text{Br-Br})/k = 218.0 \text{ K}, \quad \sigma(\text{Br-Br}) = 3.9 \text{ \AA}, \quad q_{\text{Br}} = -0.160 |e|,$$

$$\epsilon(\text{Cl-Cl})/k = 158.0 \text{ K}, \quad \sigma(\text{Cl-Cl}) = 3.6 \text{ \AA}, \quad q_{\text{Cl}} = -0.180 |e|,$$

$$\epsilon(\text{F-F})/k = 54.9 \text{ K}, \quad \sigma(\text{F-F}) = 2.7 \text{ \AA}, \quad q_{\text{F}} = -0.22 |e|.$$

The simulation was carried out: (i) for 108 (*R*) and (*S*) CHBrClF molecules; and (ii) 54 molecules each of (*R*) and (*S*) CHBrClF—the racemic mixture. The input temperature was 296 K and input molar volume  $1.20 \times 10^{26}$  Å<sup>3</sup>/mole. The site-site parameters were taken from the literature, and assumed to be the same for both *R-R* and *R-S* interactions. There are no experimental indications to the contrary, because the true pair potential is unknown.

After equilibration, the autocorrelation functions of  $2m\mathbf{v} \times \boldsymbol{\omega}$ ,  $m\boldsymbol{\omega} \times (\boldsymbol{\omega} \times \mathbf{r})$ , and  $m\mathbf{r} \times \dot{\boldsymbol{\omega}}$  were evaluated with running-time averages in the usual way, using 1000 time-step segments (500 records separated by 0.01 ps). Cross-correlation functions were evaluated as for dichloromethane using this method.

## C. Results and discussion

### 1. Liquid dichloromethane: field off

The autocorrelation function of the Coriolis acceleration,  $2\boldsymbol{\omega} \times \mathbf{v}$ , exists in both the laboratory and moving frames of reference, and these are illustrated in Fig. 1. Similarly (Fig. 2), the autocorrelation functions of the centripetal acceleration,  $\boldsymbol{\omega} \times (\boldsymbol{\omega} \times \mathbf{r})$ , and of the acceleration  $\dot{\boldsymbol{\omega}} \times \mathbf{r}$  (Fig. 3) exist in both frames, the former reaches a plateau level as  $t \rightarrow \infty$  and the latter has a negative overshoot. These autocorrelation functions in themselves provide new ways of correlating statistically rotational motion and translational motion, through the intermediacy of the angular velocity  $\boldsymbol{\omega}$ , its derivative  $\dot{\boldsymbol{\omega}}$ , translational velocity  $\mathbf{v}$ , and the center-of-mass position vector  $\mathbf{r}$ .

Curves 1 and 2 of Figs. 1 and 2 are different in time dependence because they are compared in different frames of reference (*x,y,z*) and (1,2,3) for an asymmetric top. The frame-transformation relations near components of any such ACF in the moving frame will not be isotropic in time dependence, in contrast to their counterparts in frame (*x,y,z*). The curves 1 and 2 would be identical for a spherical top.

It is difficult to find in the literature much reference, if any, to the role of the position vector  $\mathbf{r}$  in the analytical theory<sup>2,28</sup> based on the single-particle Langevin equation.

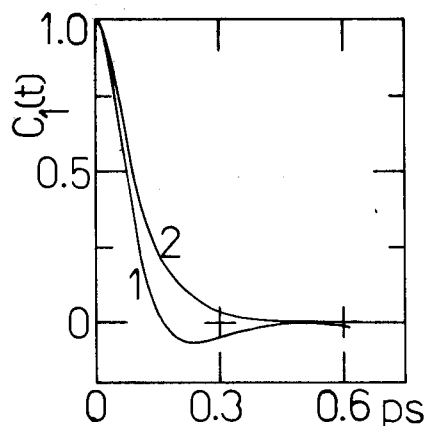


FIG. 1. Autocorrelation functions of the molecular Coriolis force, normalized to unity at  $C_1(t) = \langle 2\mathbf{v}(t) \times \boldsymbol{\omega}(t) \cdot 2\mathbf{v}(0) \times \boldsymbol{\omega}(0) \rangle / \langle [2\mathbf{v}(0) \times \boldsymbol{\omega}(0)]^2 \rangle$ . 1, frame (*x,y,z*); 2, frame (1,2,3). Dichloromethane liquid, field off.

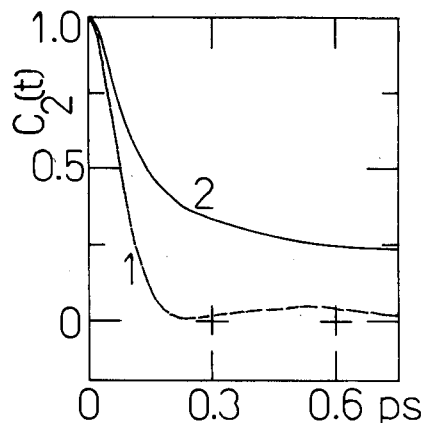


FIG. 2. Autocorrelation functions  $C_2(t)$  of the molecular centripetal force, normalized to unity at the origin. 1, frame (1,2,3); 2, frame (*x,y,z*). Dichloromethane, field off.

$$C_2(t) = \frac{\langle \boldsymbol{\omega}(t) \times [\boldsymbol{\omega}(t) \times \mathbf{r}(t)] \cdot \boldsymbol{\omega}(0) \times [\boldsymbol{\omega}(0) \times \mathbf{r}(0)] \rangle}{\langle \{\boldsymbol{\omega}(0) \times [\boldsymbol{\omega}(0) \times \mathbf{r}(0)]\}^2 \rangle}$$

The vast majority of papers deals with the rotational equation alone, where  $\mathbf{r}$  is undefined, or the translational equation, where it appears only through a conjugate variable, its time derivative  $\mathbf{v}$ . In the translational approach  $\boldsymbol{\omega}$  is undefined. Figures 1–3 now show that the three acceleration terms introduced by a full consideration of the trajectory in three dimensions of the asymmetric top have their own autocorrelation functions whose time dependence is determined by the various types of statistical correlation between translation and rotation.

Therefore to bridge the gap between molecular dynamics<sup>2,8,28</sup> and hydrodynamics<sup>3,5,6,13</sup> requires full consideration of these *basic*, single-molecule properties before proceeding to more complicated *N*-molecule dynamics.

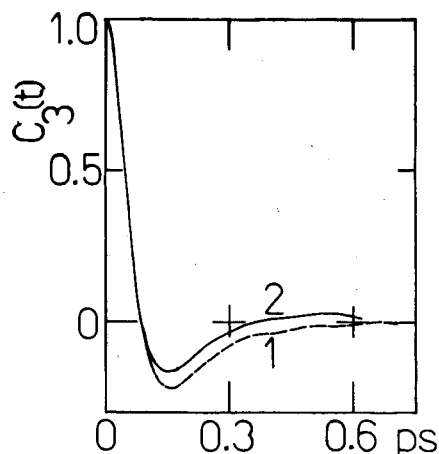


FIG. 3. Autocorrelation functions  $C_3(t)$  of the molecular force  $\dot{\boldsymbol{\omega}} \times \mathbf{r}$ , due to the nonuniformity of the molecule's rotational motion. In the actual examples here  $\dot{\boldsymbol{\omega}}$  has been replaced by the torque ( $T_q$ ) for computational convenience. 1, frame (*x,y,z*); 2, frame (1,2,3). Normalization to unity at the origin. Dichloromethane, field off.

$$C_3(t) = \frac{\langle \dot{\boldsymbol{\omega}}(t) \times \mathbf{r}(t) \cdot \dot{\boldsymbol{\omega}}(0) \times \mathbf{r}(0) \rangle}{\langle [\dot{\boldsymbol{\omega}}(0) \times \mathbf{r}(0)]^2 \rangle}$$

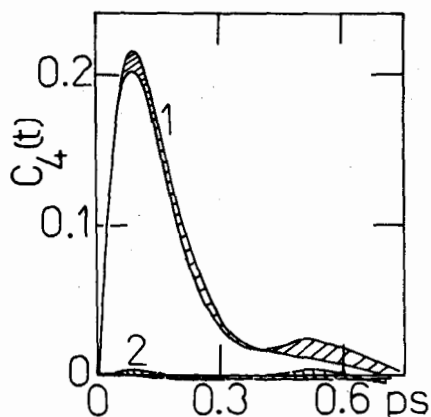


FIG. 4. The cross-correlation function  $C_4(t) = \langle \omega(t) \times v(t) \cdot v(0) \rangle / \langle \omega^2 \rangle^{1/2} \langle v^2 \rangle$ . 1, frame (1,2,3); 2, frame (x,y,z). The hatching here and in the following figures denotes the difference between two segments of 2700 time steps each. Dichloromethane, field off.

This can be done straightforwardly with computer simulation, which can be used to look at the ten cross-correlation functions denoted (i)–(x) earlier in this paper. In this way it is possible to discern which exist and which vanish, presumably by parity symmetry.<sup>6,13</sup> The type of normalization used in (i)–(x) is necessitated by the fact that these cross-correlation functions all vanish in both frames at  $t=0$ . The following results then appear from the simulation in the field-off case.

(1) Most of the cross-correlation functions vanish in the computer noise in both frames of reference but the following exist and are illustrated in Figs. 4–7.

(2) The cross-correlation function

$$C_{(iii)}(t) = \frac{\langle 2\omega(t) \times v(t) \cdot v(0) \rangle}{2\langle \omega^2(0) \rangle^{1/2} \langle v^2(0) \rangle}$$

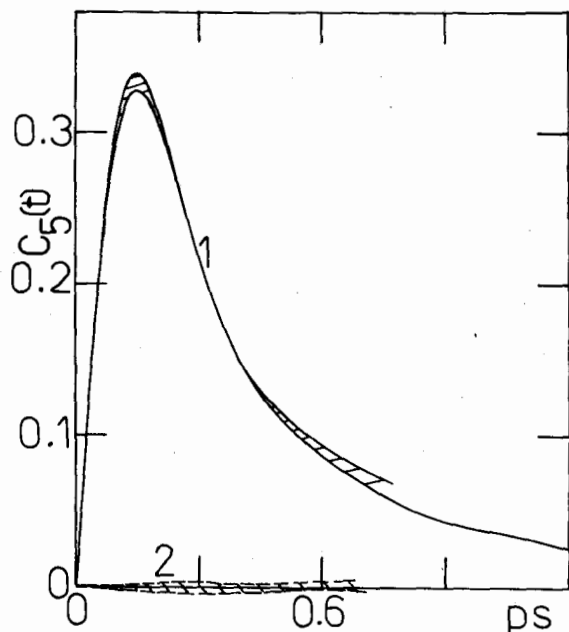


FIG. 5. As for Fig. 4,  $C_5(t) = \langle \omega(t) \times r(t) \cdot r(0) \rangle / \langle \omega^2 \rangle^{1/2} \langle r^2 \rangle$ .

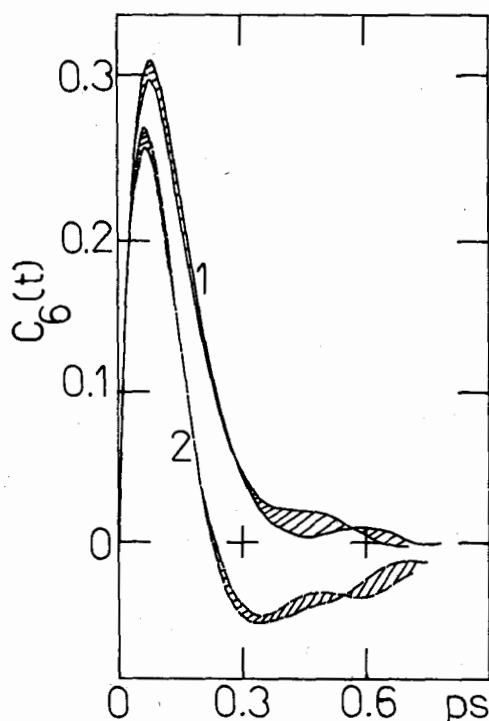


FIG. 6. The cross-correlation function

$$C_6(t) = \frac{\langle r(t) \times \omega(t) \cdot T_q(0) \times r(0) \rangle}{\langle r^2 \rangle \langle \omega^2 \rangle^{1/2} \langle T_q^2 \rangle^{1/2}}$$

Dichloromethane liquid, field-off.

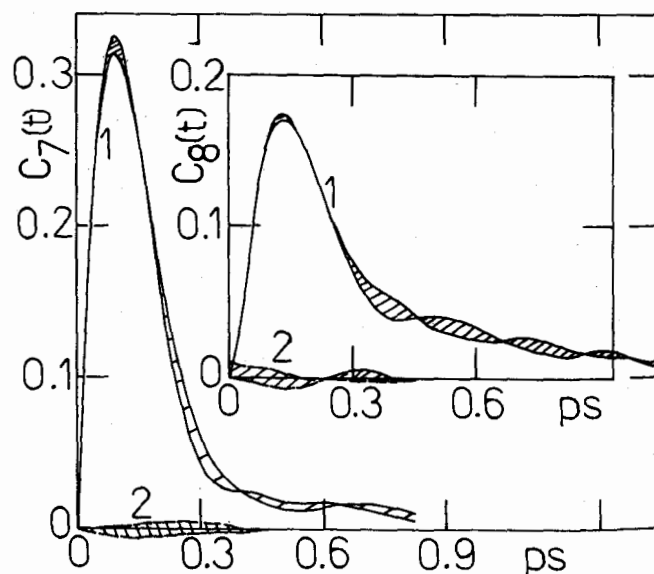


FIG. 7. The cross-correlation function

$$C_7(t) = \frac{\langle r(t) \times \omega(t) \cdot \omega(0) \times [\omega(0) \times r(0)] \rangle}{\langle r^2 \rangle \langle \omega^2 \rangle \langle \omega^2 \rangle^{1/2}}$$

1, frame (1,2,3); 2, frame (x,y,z). Inset: The cross-correlation function

$$C_8(t) = \frac{\langle T_q(t) \times r(t) \cdot \omega(0) \times [\omega(0) \times r(0)] \rangle}{\langle T_q^2 \rangle^{1/2} \langle r^2 \rangle \langle \omega^2 \rangle}$$

1, frame (1,2,3); 2, frame (x,y,z). Dichloromethane liquid, field off.

exists in the frame (1,2,3) of the molecular principal moments of inertia but vanishes in the laboratory frame ( $x,y,z$ ). Figure 4 shows two ACF's computed with two different segments of 900 records each (2700 time steps). The difference between two segments is one acceptable indication of the level of noise, and this is the hatched area in Fig. 4. The function  $C_{(iii)}$  is therefore an interesting new way of looking at field-off cross correlation in the moving frame (1,2,3). In this respect it supplements moving frame ACF's

$$C_{v\omega} = \langle v(t)\omega^T(0) \rangle_{MF}$$

used in Eqs. (1) and (2). Up to now this function seems to have been the only way of measuring<sup>18</sup> cross correlation of this type on a single-molecule level.

For  $\text{CH}_2\text{Cl}_2$  liquid at 296 K the function  $C_{(iii)}$  in the moving frame of reference (1,2,3), reaches a maximum of  $0.205 \pm 0.05$  within the noise, and has a positive nonvanishing slope as  $t \rightarrow 0$ , unlike the function  $C_{v\omega}$ . Physically, it measures the statistical time correlation between the Coriolis acceleration at a time  $t$  and the center-of-mass linear velocity at  $t=0$  for the same molecule.

In this context it is interesting to note that the superficially similar cross-correlation functions (a)  $\langle \omega(t) \times v(t) \cdot \omega(0) \rangle$ , (b)  $\langle \dot{\omega}(t) \times r(t) \cdot v(0) \rangle$ , (c)  $\langle \omega(t) \times r(t) \cdot v(0) \rangle$ , and (d)  $\langle v(t) \times \omega(t) \cdot r(0) \rangle$  vanish in both frames of reference, but the correlation function

$$C_{rr} = \frac{\langle \omega(t) \times r(t) \cdot r(0) \rangle}{\langle \omega^2 \rangle^{1/2} \langle r^2 \rangle}$$

exists in the moving frame (Fig. 5) and vanishes only in the laboratory frame ( $x,y,z$ )

The moving frame  $C_{rr}$  attains a maximum of  $(0.330 \pm 0.005)$  at 0.15 ps, and seems to be longer lived than its equivalent in Fig. 4. Again the cross-correlation function does not have a zero slope at  $t=0$ .

There is a class of cross-correlation functions which exist in both frames of reference, and this is typified by

$$C_{(vii)} = \frac{\langle r(t) \times \omega(t) \cdot \dot{\omega}(0) \times r(0) \rangle}{\langle r^2 \rangle \langle \omega^2 \rangle^{1/2} \langle \dot{\omega}^2 \rangle^{1/2}}$$

which is illustrated in Fig. 6. [In the actual computation in Fig. 6  $\dot{\omega}(0)$  was replaced for convenience by the torque vector.] In physical terms  $C_{(vii)}$  is the cross correlation between the velocity  $r \times \omega$  and the acceleration  $\dot{\omega} \times r$  due to the nonuniformity of the angular motion of the molecule.

Finally Fig. 7 demonstrates the existence of

$$C_{(ix)} = \frac{\langle r(t) \times \omega(t) \cdot \omega(0) \times [\omega(0) \times r(0)] \rangle}{\langle r^2 \rangle \langle \omega^2 \rangle \langle \omega^2 \rangle^{1/2}}$$

in the rotating frame (1,2,3), but not in the laboratory frame.

## 2. Field-on cross-correlation functions

It is known<sup>14,22</sup> that the application of an external field of force results in the appearance of two new off-diagonal elements of the matrix  $\langle v(t)\omega^T(0) \rangle$  in the laboratory frame of reference, thus invalidating the field-off theorem<sup>6</sup> (2). In this section an external electric field is

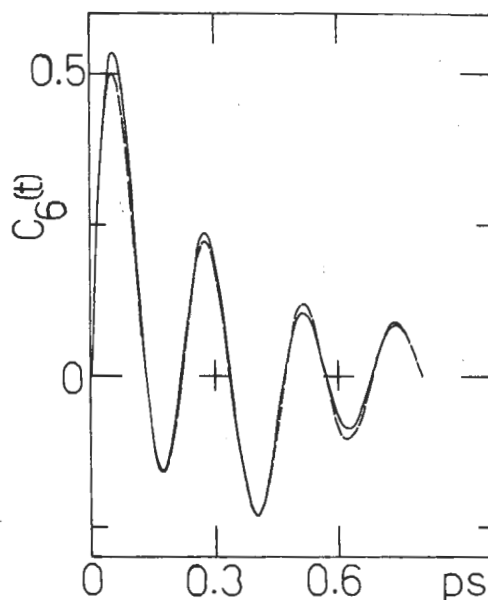


FIG. 8. As for Fig. 6, dichloromethane, field on. —, frame ( $x,y,z$ ); ---, frame (1,2,3).

applied in the  $z$  axis of the laboratory frame ( $x,y,z$ ) strong enough nearly to saturate the Langevin function.<sup>16,22</sup> At field-on equilibrium the average  $\langle e_{3z} \rangle$ , for example, is  $(0.93 \pm 0.02)$ . Here  $e_3$  is a unit vector in the 3 axis of frame (1,2,3) and  $e_{3z}$  is its  $z$  component in frame ( $x,y,z$ ). The result  $\langle e_{3z} \rangle = 0.93$  means that there is significant alignment of the 108 molecules produced by the applied electric field. This section deals with the effect of this alignment on cross-correlation functions of the type introduced in Sec. II.

The cross-correlation function (vii) is affected (Fig. 8) in such a way that its behavior in frames (1,2,3) and ( $x,y,z$ ) becomes almost identical. In comparison with Fig. 6 the envelope of the oscillations introduced by the electric field survives for a longer time. This can be understood in terms of the Grigolini decoupling effect,<sup>29</sup>

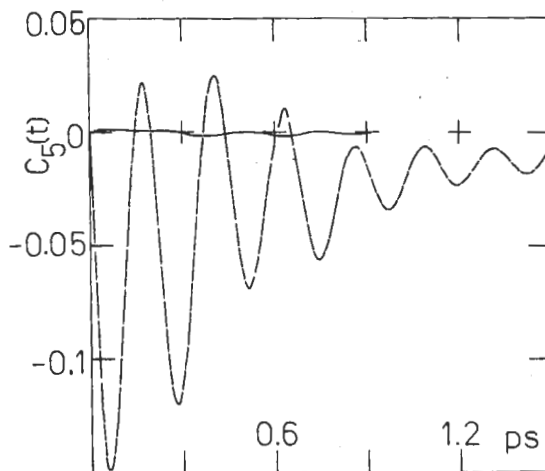


FIG. 9. As for Fig. 5, dichloromethane, field on. ---, frame (1,2,3); —, frame ( $x,y,z$ ). [In this figure, we have used the triple product  $r(t) \times \omega(t) \cdot r(0)$ , which accounts for the sign reversal in the frame (1,2,3).]



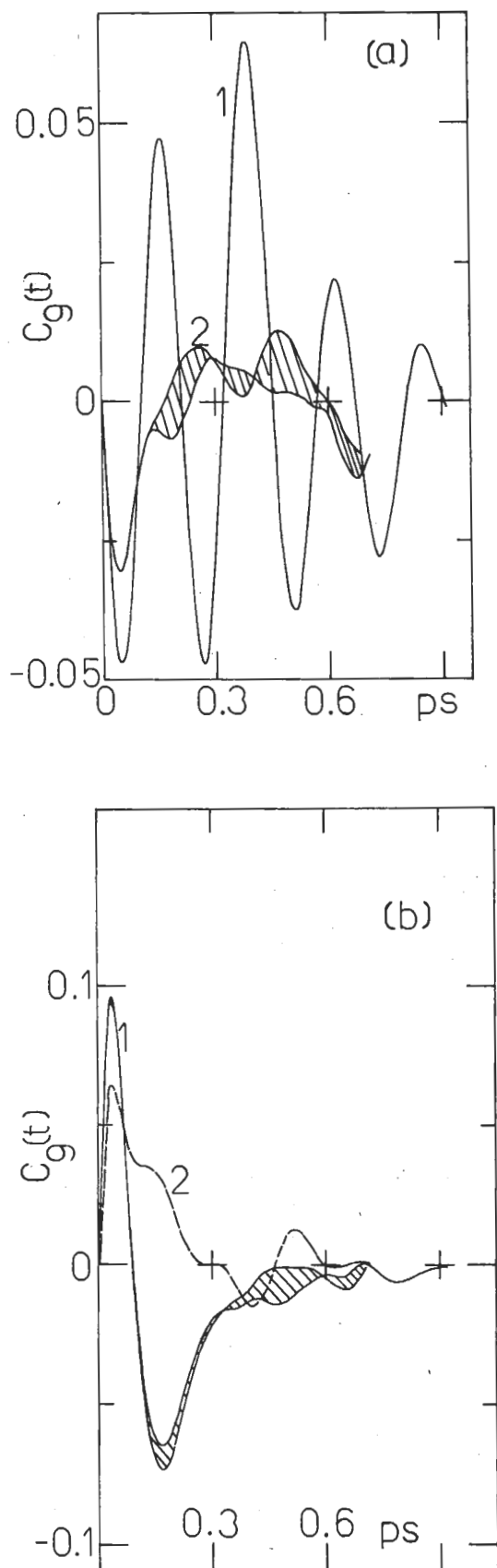


FIG. 10. (a) The cross-correlation function  $C_g(t) = \langle \omega(t) \times \mathbf{T}_g(t) \cdot \mathbf{T}_g(0) \rangle / \langle \omega \rangle^{1/2} \langle \mathbf{T}_g^2 \rangle$  in the frame  $(x,y,z)$ . Dichloromethane liquid; 1, field on; 2, field off. (b) As for (a), frame  $(1,2,3)$ .

well known for autocorrelation functions.

The effect of the electric field on cross-correlation functions of the general type  $C_A(t) = \langle \mathbf{A}(t) \times \omega(t) \cdot \mathbf{A}(0) \rangle / (\langle A^2 \rangle \langle \omega^2 \rangle^{1/2})$  is exemplified for  $\mathbf{A} \equiv \mathbf{r}$  in Fig. 9. The equivalent field-off case is Fig. 5. The cross-correlation function in Fig. 9 exists in frame  $(1,2,3)$  but *disappears* for all  $t$  in frame  $(x,y,z)$ . This is the same overall result as in Fig. 5, which suggests that the *same* overall symmetry law governs the time dependence of such cross-correlation functions in the presence *and* absence of the electric field  $\mathbf{E}$ . This law is different from that governing the existence of  $\langle \mathbf{v}(t) \omega^T(0) \rangle$ , which vanishes in the absence of  $\mathbf{E}$  but exists in its presence for frame  $(x,y,z)$  and always exists in frame  $(1,2,3)$ .

When  $\mathbf{A} \equiv \mathbf{T}_g$  [Figs. 10(a) and 10(b)], where  $\mathbf{T}_g$  denotes the net torque on a molecule at time  $t$ , the effect of an applied  $z$ -axis electric field is to enhance the (very small) amplitude of this cross-correlation function in frame  $(x,y,z)$ , which is barely visible in the absence of the field. Again the Grigolini decoupling effect<sup>29</sup> is observable in the envelope of the oscillations introduced by this field.<sup>30</sup> There is a similar effect in frame  $(1,2,3)$  [Fig. 10(b)] where the amplitude of the cross-correlation function is greater both in the presence and absence of the field.

The subtle effects of symmetry can be seen clearly in Fig. 11(a). This figure illustrates in curve (1) the cross-correlation function in frame  $(1,2,3)$  for  $\mathbf{A} = \mathbf{v}$ , the center-of-mass velocity. As in Fig. 4 this cross-correlation function exists in frame  $(1,2,3)$  and vanishes in frame  $(x,y,z)$ . This follows the rule that  $C_A(t)$  exists in frame  $(1,2,3)$  and vanishes in frame  $(x,y,z)$  *both* in the presence *and* absence of a  $z$ -axis electric field.

In contrast, curve (2) of Fig. 11(a) illustrates the fact that the cross-correlation function  $\langle \omega(t) \times \mathbf{v}(t) \cdot \omega(0) \rangle$  *vanishes* for all  $t$  *both* in frame  $(1,2,3)$  *and*  $(x,y,z)$  in the absence *and* presence of the electric field. Therefore,

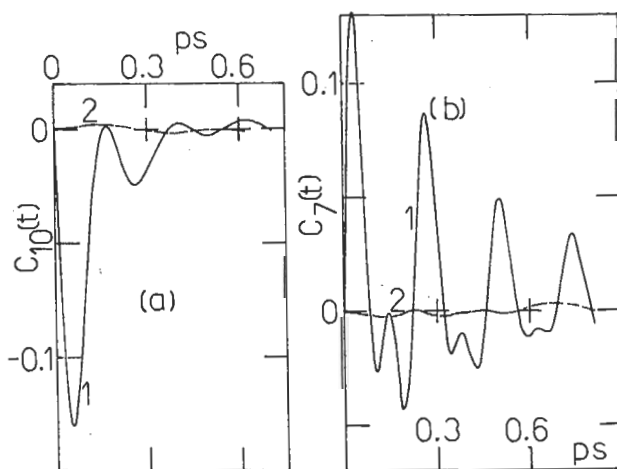


FIG. 11. Dichloromethane, field on. (a) The cross-correlation function  $C_{10}(t) = \langle \mathbf{v}(t) \times \omega(t) \cdot \mathbf{v}(0) \rangle / \langle v^2 \rangle \langle \omega^2 \rangle^{1/2}$ . 1, frame  $(1,2,3)$ ; 2, frame  $(x,y,z)$ . (b)

$$C_7(t) = \frac{\langle \mathbf{r}(t) \times \omega(t) \cdot \omega(0) \times [\omega(0) \times \mathbf{r}(0)] \rangle}{\langle r^2 \rangle \langle \omega^2 \rangle \langle \omega^2 \rangle^{1/2}}$$

1, frame  $(1,2,3)$ ; 2, frame  $(x,y,z)$ .

there exists a statistical cross correlation between the Coriolis acceleration and the *linear* velocity  $\mathbf{v}$  in frame (1,2,3), but there is *never* any cross correlation between the Coriolis acceleration and the *angular* velocity  $\boldsymbol{\omega}$  in any frame of reference, either in the absence or presence of an external electric field.

The pattern is repeated for the type  $C_A(t)$  in Fig. 11(b), where  $\mathbf{A} \equiv \boldsymbol{\omega} \times \mathbf{r}$ . The field-off equivalent to Fig. 11(b) is Fig. 7. In both figures the cross-correlation function exists in frame (1,2,3) but vanishes for all  $t$  in frame  $(x,y,z)$ . The field-induced oscillations in Fig. 11(b) show an interesting pattern of alternate large-amplitude and small-amplitude peaks. The overall envelope of these field-induced oscillations follow the Grigolini decoupling rule<sup>29</sup> in being longer lived than the field-off equivalent in frame (1,2,3) (Fig. 7).

None of these cross-correlation functions are described by state-of-the-art<sup>8</sup> analytical theories of decoupled rotational or translational molecular diffusion in *any* frame of reference. This shows how much information is lost by

the traditional one-particle approach, and leads us to question its usefulness *vis à vis* computer simulation. Analytical methods of solving Eqs. (3) and (5) of Sec. I are necessary to begin to remedy this problem.

The symmetry properties of the cross-correlation functions are summarized in Table I, where a plus sign denotes the existence of the ACF for  $t > 0$ . The ACF's fall into various classes or types, and five types are exemplified in the table. It is interesting in this context to compare types II and V, a tensor ACF and vector ACF respectively. It is known<sup>12,18</sup> that the off-diagonal elements of  $\langle \mathbf{v}(t)\boldsymbol{\omega}^T(0) \rangle$  exist for  $t > 0$ , but the diagonal elements all vanish, so that the "trace"  $\langle \mathbf{v}(t) \cdot \boldsymbol{\omega}(0) \rangle$  also vanishes. This has been confirmed independently in this work and reported in Table I as type V. The importance of this comparison is that off-diagonal elements of the tensor products equivalent to the vector products in Table I may exist for  $t > 0$ , providing a very large number of new ways of correlating the various types of motion in a molecular liquid.

TABLE I. Symmetry classification of cross-correlation functions: Achiral asymmetric tops ( $\text{CH}_2\text{Cl}_2$ ). All the autocorrelation functions of the vectors in this table exist in both frames for  $\mathbf{E} > 0$ .

Type	Examples	(x,y,z)	(1,2,3)	(x,y,z)+E	(1,2,3)+E
I	$\frac{\langle \mathbf{r}(t) \times \boldsymbol{\omega}(t) \cdot \dot{\boldsymbol{\omega}}(0) \times \mathbf{r}(0) \rangle}{\langle r^2 \rangle \langle \omega^2 \rangle^{1/2} \langle \dot{\omega}^2 \rangle^{1/2}}$ $\frac{\langle \boldsymbol{\omega}(t) \times \dot{\boldsymbol{\omega}}(t) \cdot \dot{\boldsymbol{\omega}}(0) \rangle}{\langle \omega^2 \rangle^{1/2} \langle \dot{\omega}^2 \rangle}$	+	+	+	+
II	$\frac{\langle \mathbf{v}(t)\boldsymbol{\omega}^T(0) \rangle}{\langle \mathbf{v}(0)\boldsymbol{\omega}^T(0) \rangle}$	-	+	+	+
III	$\frac{\langle \mathbf{A}(t) \times \boldsymbol{\omega}(t) \cdot \mathbf{A}(0) \rangle}{\langle A^2 \rangle \langle \omega^2 \rangle^{1/2}}$ ( $\mathbf{A} \equiv \mathbf{v}; \boldsymbol{\omega} \times \mathbf{r}; \mathbf{r}$ ) $\frac{\langle \dot{\boldsymbol{\omega}}(t) \times \mathbf{r}(t) \cdot \boldsymbol{\omega}(0) \times [\boldsymbol{\omega}(0) \times \mathbf{r}(0)] \rangle}{\langle \dot{\omega}^2 \rangle^{1/2} \langle \omega^2 \rangle \langle r^2 \rangle}$	-	+	-	+
IV	$\frac{\langle \boldsymbol{\omega}(t) \times \mathbf{v}(t) \cdot \boldsymbol{\omega}(0) \rangle}{\langle \omega^2 \rangle \langle v^2 \rangle^{1/2}}$ $\frac{\langle \mathbf{v}(t) \times \boldsymbol{\omega}(t) \cdot \mathbf{r}(0) \rangle}{\langle v^2 \rangle^{1/2} \langle \omega^2 \rangle^{1/2} \langle r^2 \rangle^{1/2}}$ $\frac{\langle \dot{\boldsymbol{\omega}}(t) \times \mathbf{r}(t) \cdot \mathbf{v}(0) \rangle}{\langle \dot{\omega}^2 \rangle^{1/2} \langle r^2 \rangle^{1/2} \langle v^2 \rangle^{1/2}}$ $\frac{\langle \boldsymbol{\omega}(t) \times \mathbf{r}(t) \cdot \mathbf{v}(0) \rangle}{\langle \omega^2 \rangle^{1/2} \langle r^2 \rangle^{1/2} \langle v^2 \rangle^{1/2}}$ $\frac{\langle \mathbf{v}(t) \times \boldsymbol{\omega}(t) \cdot \dot{\boldsymbol{\omega}}(0) \times \mathbf{r}(0) \rangle}{\langle v^2 \rangle^{1/2} \langle \omega^2 \rangle^{1/2} \langle \dot{\omega}^2 \rangle^{1/2} \langle r^2 \rangle^{1/2}}$ $\frac{\langle \mathbf{v}(t) \times \boldsymbol{\omega}(t) \cdot \boldsymbol{\omega}(0) \times \mathbf{r}(0) \rangle}{\langle v^2 \rangle^{1/2} \langle \omega^2 \rangle \langle r^2 \rangle^{1/2}}$ $\frac{\langle \boldsymbol{\omega}(t) \times [\boldsymbol{\omega}(t) \times \mathbf{r}(t)] \cdot \mathbf{v}(0) \rangle}{\langle \omega^2 \rangle \langle r^2 \rangle^{1/2} \langle v^2 \rangle^{1/2}}$ $\frac{\langle \mathbf{v}(t) \times \boldsymbol{\omega}(t) \cdot \boldsymbol{\omega}(0) \times [\boldsymbol{\omega}(0) \times \mathbf{r}(0)] \rangle}{\langle v^2 \rangle^{1/2} \langle \omega^2 \rangle^{1/2} \langle \omega^2 \rangle \langle r^2 \rangle^{1/2}}$	-	-	-	-
V	$\frac{\langle \mathbf{v}(t) \cdot \boldsymbol{\omega}(0) \rangle}{\langle v^2 \rangle^{1/2} \langle \omega^2 \rangle^{1/2}}$	-	-	-	-

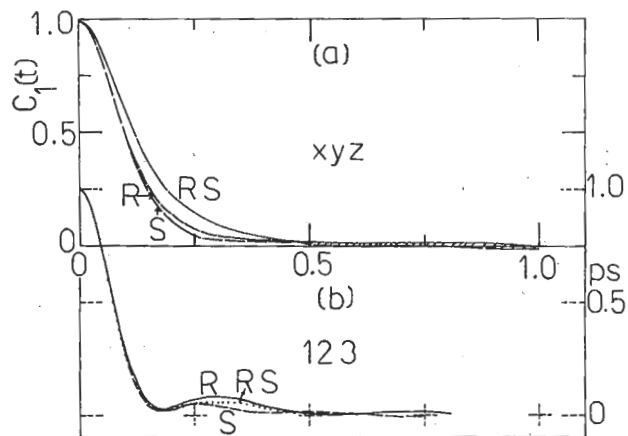


FIG. 12. Autocorrelation functions of the molecular Coriolis force, liquid bromochlorofluoromethane. (a) Frame  $(x,y,z)$ , the  $R$  and  $S$  enantiomers and  $(RS)$ , the racemic mixture. State point is 296 K, molar volume is  $1.20 \times 10^{26} \text{ \AA}^3/\text{mole}$ . (b) As for (a), frame  $(1,2,3)$ . State point is 158 K, molar volume is  $0.70 \times 10^{26} \text{ \AA}^3/\text{mole}$ .

### 3. Chiral molecules:

#### The bromochlorofluoroemethanes (Ref. 22)

Figures 12–14 illustrate the behavior at two state points of the autocorrelation functions in frame  $(x,y,z)$  of the Coriolis, centripetal, and nonuniform accelerations, respectively. These agree satisfactorily for the  $R$  and  $S$  enantiomers and differ significantly at one state point for the racemic mixture. Figure 12–14 show that these autocorrelation functions again exist in both frames:  $(x,y,z)$  and  $(1,2,3)$ .

Small differences between enantiomers and racemic mixture are observed in the other types of cross correlation noted in Table I for achiral dichloromethane liquid, significantly in the type exemplified by  $\langle \mathbf{v}(t) \times \boldsymbol{\omega}(t) \cdot \mathbf{v}(0) \rangle / (\langle v^2 \rangle \langle \omega^2 \rangle^{1/2})$  [Fig. (15)] in the moving frame of reference. The curves of Fig. 15 should be

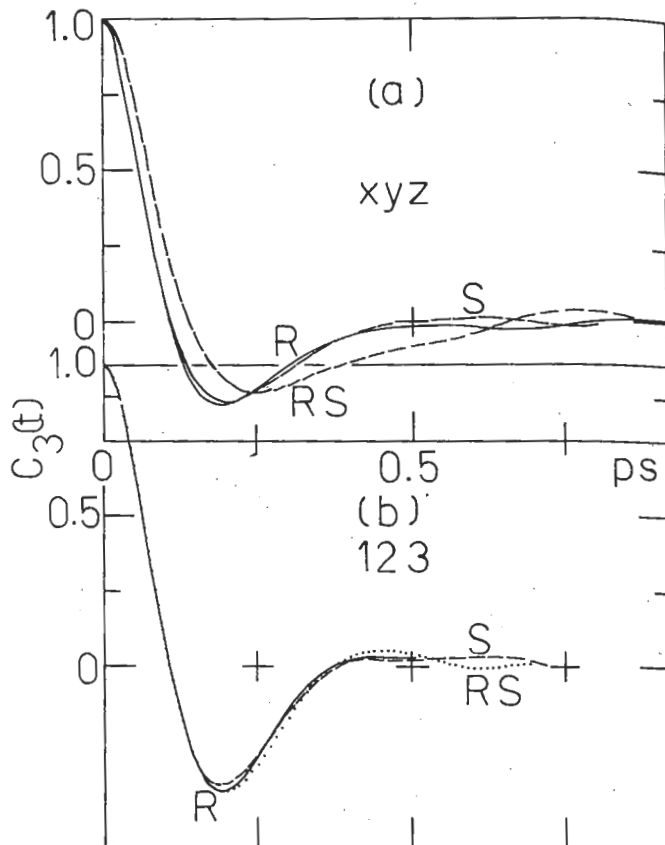


FIG. 14. As for Fig. 12, the molecular force  $T_q \times r$ .

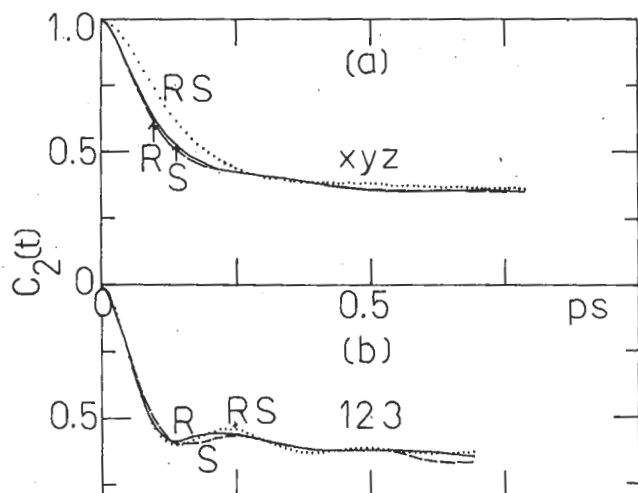


FIG. 13. As for Fig. 12, molecular centripetal force.

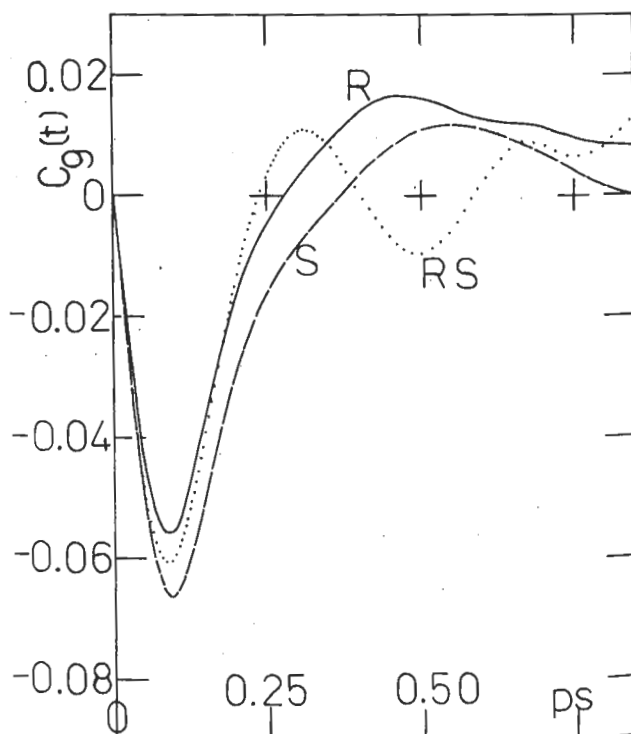


FIG. 15. The cross-correlation function  $C_9(t) = \langle \mathbf{v}(t) \times \boldsymbol{\omega}(t) \cdot \mathbf{v}(0) \rangle / (\langle v^2 \rangle \langle \omega^2 \rangle^{1/2})$  simulated for the bromochlorofluoromethanes at 158 K, molar volume is  $0.70 \times 10^{26} \text{ \AA}^3/\text{mole}$ : one segment only, for each enantiomer and the racemic mixture of 1000 time steps of 5.0 fs each.

compared with their equivalents for dichloromethane in Fig. 4. The overall symmetry pattern is the same, i.e., ACF exists in frame (1,2,3) but vanishes in frame ( $x,y,z$ ), and this is true in general for all the types of ACF's in Table I. That is to say, the overall symmetry classification in Table I is valid both for chiral and achiral asymmetric tops. However, the situation for tensor ACF's such as  $\langle v(t)\omega^T(0) \rangle$  would be significantly different.

Figure 15 shows that the vector ACF's illustrated there seem to be different for enantiomer and racemic mixture in frame (1,2,3). This type vanishes in both enantiomers and mixture in frame ( $x,y,z$ ).

Finally in this section similar results are illustrated in Fig. 16 for one other type of vector ACF that exists in frame (1,2,3). The overall (field-off) pattern is similar to that for the achiral dichloromethane summarized in Table I. There does not seem to be an accessible analytical method in the literature with which to follow these results, and it is necessary to devise a method for solving our new equations (3) and (5) for this purpose. The computer based "semianalytical" technique of "Langevin dynamics" (not to be confused with conventional molecular dynamics simulation<sup>1</sup>) seems to be the only way forward at present, although it might be possible to extend Morita's fully analytical *tour de force* solution<sup>31</sup> of Eqs. (3) to involve the extra equation (5). This contemporary lack of analytical technique highlights the role of computer simulation in describing with increased precision the molecular dynamics of the condensed phases of matter.

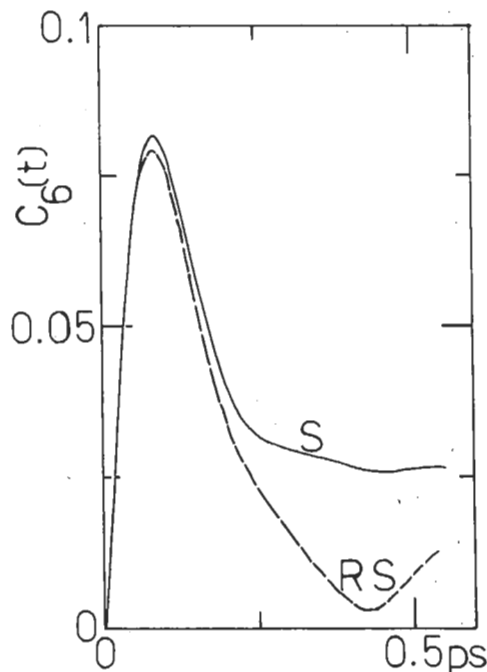


FIG. 16. The cross-correlation function

$$C_6(t) = \frac{\langle \mathbf{r}(t) \times \boldsymbol{\omega}(t) \cdot \boldsymbol{\omega}(0) \times [\boldsymbol{\omega}(0) \times \mathbf{r}(0)] \rangle}{\langle r^2 \rangle \langle \omega^2 \rangle \langle \omega^2 \rangle^{1/2}}$$

for the *S* enantiomer and racemic mixture.

### III. EXPERIMENTAL METHODS

The results from computer simulation described in this paper may be taken as a "numerical paradigm," i.e., an elaborate hypothesis, but one still needing experimental confirmation. The original hypothesis<sup>28</sup> of Langevin's diffusional equation received support—in the first half of this century, support now known<sup>18</sup> to be superficial—from data such as dielectric loss<sup>2</sup> and its frequency dependence. However, the emergence of, literally, many hundreds of highly selective cross-correlation functions, as demonstrated in this paper, requires a careful reappraisal of the original Langevin hypothesis. One of the first questions to be asked is how will it be possible to measure cross correlations experimentally, i.e., how do we isolate the specific effect of statistical cross correlation of this type from the ever-present autocorrelations of "primary" dynamical variables such as  $v$  and  $\omega$ . In this section we consider two methods and provide experimental data from one.

1. *Comparison of enantiomers and their racemic mixture.* As mentioned already this is general and easy to apply, and is therefore a potentially powerful way of establishing the nature of statistical cross correlation. The physical properties of enantiomers and their racemic mix-

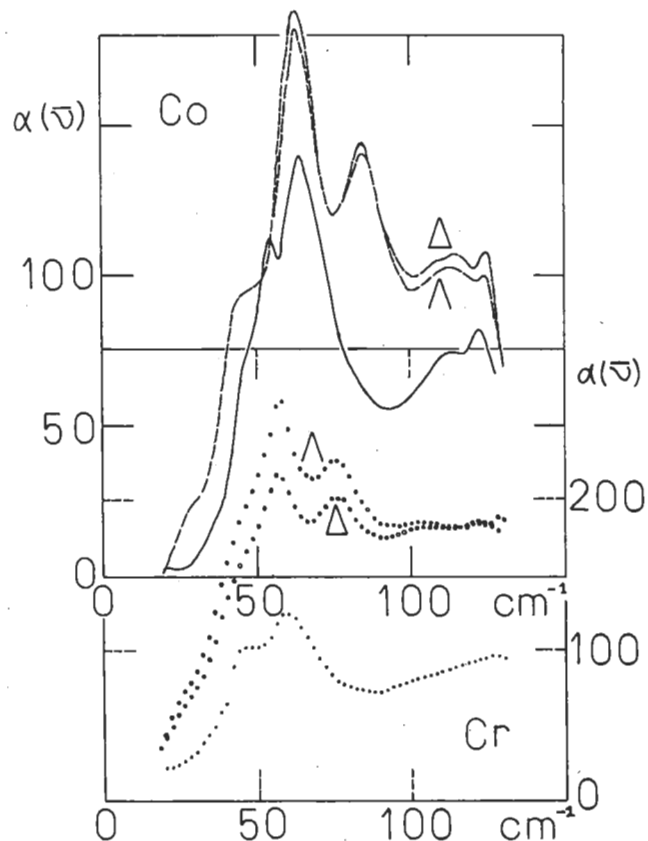


FIG. 17. Far-infrared power-absorption coefficient (in neper  $\text{cm}^{-1}$ ) for the  $\Lambda$  and  $\Delta$  enantiomers of powdered crystalline tris(acetylacetonate) complexes of cobalt and chromium in the powdered crystalline state at  $4 \text{ cm}^{-1}$  resolution. The lowest curve in each case is for the racemic mixture.

ture are, of course, well known, and well known to be different,<sup>21</sup> but it requires the additional realization that these differences are due *specifically* to statistical cross correlation before progress can be made *in the context of molecular dynamics*. There is no method of accounting for this difference using Langevin's original approach, represented for rotational diffusion<sup>2</sup> in Eq. (3). The existence of this difference implies that molecular diffusion can *never* be purely rotational or purely translational.

However, to interpret an experimental spectrum such as that illustrated in Figs. 17 and 18 in terms of cross-correlation functions between rotation and translation is a task requiring the immediate aid of computer simulation, because, as we have mentioned, there is no adequate contemporary analytical technique.

Figure 17 is a careful comparison of the far infrared power absorption coefficient<sup>2</sup> of the  $\Lambda$  and  $\Delta$  enantiomers of metal complexes with their racemic mixture in the powdered crystalline state. Examples are provided for the tris acetylacetonate complexes of cobalt and chromium at 4 cm<sup>-1</sup> resolution. A more precise comparison is made at 1 cm<sup>-1</sup> resolution for the cobalt complexes in Fig. 18. These spectra were taken on carefully prepared samples with a Crubb-Parsons/NPL "cube" interferometer,<sup>2</sup> at room temperature.

The obvious differences between the power absorption of the racemic mixture and of each enantiomer (whose spectra are identical within the experimental uncertainty and in which there is an extra phonon mode) would be interpreted traditionally in terms of the different packing symmetry.<sup>21</sup> However, in terms of molecular dynamics, this begs the question, leaving all unanswered, because packing symmetry is a purely static concept. The *dynamical* information in these spectra is to be found in the *frequency dependence* of the power absorption coefficient,<sup>2</sup> and to describe this needs the use of statistical cross correlation between rotation and translation.

It is beyond the capability of contemporary simulation<sup>1</sup> to give a direct interpretation of Figs. 17 and 18 in this way, but this may be possible soon with a simple chiral molecular liquid such as 2 chloro-butane, where there is a 9-K range of temperature where each enantiomer is a liquid but the racemic mixture is a solid. Considerations of packing symmetry alone are insufficient to describe the molecular dynamics in this range of temperature, and in this respect, the simple Langevin hypothesis is not useful. We have to consider statistical cross correlation, and to recognize fully that the molecules rotate *and* translate. In this range of temperature the role of this type of cross correlation is therefore basic. The range of temperature between the melting points of enantiomers and racemic mixture can be as much as 42 K (in the canadines<sup>19</sup>), and as little as a tenth of a degree Kelvin or less (in the camphors). The fact that we do not know why exposes starkly the limits of our contemporary understanding of the dynamical principles of molecule diffusion.

2. *Electric-field-induced birefringence*. This method makes use of the appearance<sup>16,20</sup> of the  $(x,y)$  and  $(y,x)$

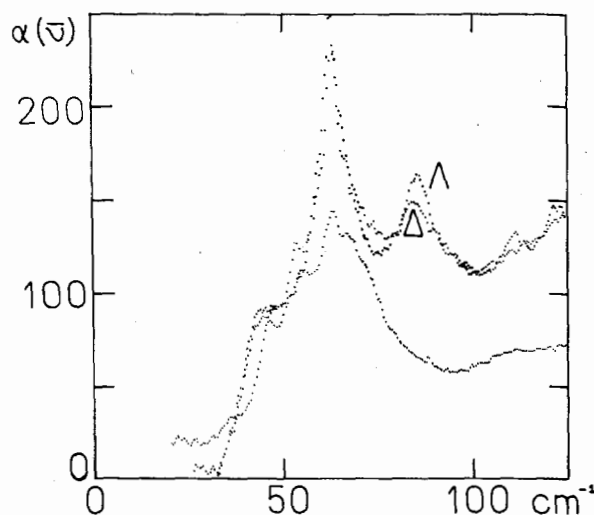


FIG. 18. As for Fig. 17, 1 cm<sup>-1</sup> resolution for the enantiomers and racemic mixture of the cobalt complex. As in Fig. 17 the lowest curve is the power absorption of the racemic mixture, which has one less phonon mode than that of either enantiomer.

components of the cross-correlation matrix  $\langle v(\tau)\omega^T(0) \rangle$  in the presence of a static electric field  $\mathbf{E}$  in the  $z$  axis of the laboratory frame. It has been shown elsewhere<sup>16</sup> that measurements of the far infrared power absorption perpendicular and parallel to the electric field leads in principle to the experimental isolation of these elemental laboratory-frame cross correlations of  $\langle v(\tau)\omega^T(0) \rangle$ , both for chiral *and* achiral asymmetric tops.

## CONCLUSIONS

A consideration of molecular diffusion involving simultaneous rotation and translation leads to a number of new correlation functions with which to describe the complete trajectory. The autocorrelation functions exist both in the laboratory  $(x,y,z)$  and moving  $(1,2,3)$  frames of reference. Some of the cross-correlation functions exist in the moving frame  $(1,2,3)$  and vanish in the laboratory frame  $(x,y,z)$ , others exist in both frames, and still others vanish in both frames. A table summarizing these symmetry properties is provided in this paper. The overall symmetry pattern in this table is similar for achiral and chiral liquids, although extra information is available from a comparison of enantiomers and racemic mixture.

By extending the analysis of Table I to tensor cross-correlation functions, several hundred new ways become available of looking at the correlations between vectors such as  $\mathbf{r}$ ,  $\mathbf{v}$ , and  $\mathbf{w}$ .

## ACKNOWLEDGMENTS

Financial support by the University of Wales and by the United Kingdom Science and Engineering Research Council (SERC) is gratefully acknowledged.

- <sup>1</sup>D. Fincham and D. Heyes, in *Dynamical Processes in Condensed Matter*, Vol. 63 of *Advances in Chemical Physics*, edited by M. W. Evans (Wiley Interscience, New York, 1985).
- <sup>2</sup>M. W. Evans, G. J. Evans, W. T. Coffey, and P. Grigolini, *Molecular Dynamics* (Wiley Interscience, New York, 1982).
- <sup>3</sup>E. Dickinson, *Chem. Brit.* **21**, 4 (1985).
- <sup>4</sup>J. K. Moscicki, in Ref. 1.
- <sup>5</sup>D. W. Condiff and J. S. Dahler, *J. Chem. Phys.* **44**, 3988 (1966).
- <sup>6</sup>B. J. Berne and R. Pecora, *Dynamical Light Scattering with Reference to Physics, Chemistry and Biology* (Wiley Interscience, New York, 1976).
- <sup>7</sup>U. Steiger and R. F. Fox, *J. Math. Phys.* **23**, 296 (1982).
- <sup>8</sup>P. Grigolini *et al.*, in *Memory Function Approaches to Stochastic Problems in Condensed Matter*, Vol. 62 of *Advances in Chemical Physics*, edited by M. W. Evans, P. Grigolini, and G. Pastori-Parravicini (Wiley Interscience, New York, 1985).
- <sup>9</sup>G. T. Evans, *Mol. Phys.* **36**, 1199 (1978).
- <sup>10</sup>L. P. Hwang and J. H. Freed, *J. Chem. Phys.* **63**, 118 (1975); **63**, 4017 (1975).
- <sup>11</sup>J. P. Ryckaert, A. Bellemans, and G. Ciccotti, *Mol. Phys.* **44**, 979 (1981).
- <sup>12</sup>M. W. Evans, *Phys. Rev. Lett.* **50**, 371 (1983).
- <sup>13</sup>N. K. Ailawadi, B. J. Berne, and D. Forster, *Phys. Rev. A* **3**, 1462 (1971); **3**, 1472 (1971).
- <sup>14</sup>M. W. Evans, *Physica B* (to be published).
- <sup>15</sup>M. R. Spiegel, *Theory and Problems of Vector Analysis* (Schaum, New York, 1959), p. 53.
- <sup>16</sup>See W. T. Coffey, M. W. Evans, and P. Grigolini, *Molecular Diffusion* (Wiley Interscience, New York, 1984), Chaps. 1–3.
- <sup>17</sup>For a review of friction cross terms, see Ref. 2, Chap. 5.
- <sup>18</sup>For a review, see M. W. Evans and G. J. Evans in Ref. 1.
- <sup>19</sup>M. W. Evans, and G. J. Evans, *Phys. Rev. Lett.* **55**, 818 (1985).
- <sup>20</sup>For a review, see Ref. 1, Chap. 4.
- <sup>21</sup>S. F. Mason, *Molecular Optical Activity and the Chiral Discrimination* (Cambridge University, Cambridge, 1982).
- <sup>22</sup>M. W. Evans, *Phys. Rev. A* **30**, 2062 (1984); **31**, 3947 (1985).
- <sup>23</sup>M. W. Evans, *Phys. Scr.* **31**, 419 (1985); *Physica B* (to be published).
- <sup>24</sup>J. Smythe, F. Moss, and P. V. E. McClintock, *Phys. Rev. Lett.* **51**, 1062 (1983).
- <sup>25</sup>P. Hanggi, T. J. Mroczkowski, F. Moss, and P. V. E. McClintock, *Phys. Rev. A* **32**, 695 (1985).
- <sup>26</sup>L. Fronzoni *et al.*, in Ref. 8, Chap. X.
- <sup>27</sup>M. W. Evans, *J. Chem. Soc., Faraday Trans. II* **79**, 1811 (1982); *J. Mol. Liq.* **27**, 11 (1983).
- <sup>28</sup>W. T. Coffey, in Ref. 1.
- <sup>29</sup>See Ref. 8, Chap. 6.
- <sup>30</sup>Ref. 16, Chaps. 7–9.
- <sup>31</sup>A. Morita, *J. Phys. D* **11**, 1357 (1978).